Morphological evolution in ballistic deposition

C. Lehnen and T.-M. Lu
Department of Physics, Applied Physics, and Astronomy, Rensselaer Polytechnic Institute, Troy, New York 12180-3590, USA
(Received 28 July 2010; published 24 August 2010)

Ballistic deposition model has been employed to simulate the morphological evolution of thin-film growth under non-normal incident flux that occurs frequently in realistic physical vapor deposition. We show that the growth front clearly deviates from the Kardar, Parisi, and Zhang universality class and the growth front exhibits a characteristic length scale that gives rise to a wavelength selection. The implication is that under realistic physical vapor deposition conditions, the growth front morphology is expected not to obey the well-established dynamic scaling hypothesis.

DOI: 10.1103/PhysRevB.82.085437 PACS number(s): 68.55.−a, 05.40.−a, 68.35.Ct, 81.15.−z

Ballistic deposition model has been used extensively in the literature to describe the evolution of a growing surface,[1,2] an important area in the development of nonequilibrium statistical mechanics. The model was originally developed by Vold to simulate the sedimentation process.[3] In its simplest form the model involves the deposition of particles randomly along the vertical trajectories onto a two-dimensional (2D) flat surface. Particles become part of the depositing aggregates at their positions of first contacts. The deposition creates a porous film with overhangs throughout the structure. A fascinating subject has been the study of the dynamic scaling and universality behavior of the morphological evolution of the film by ignoring the overhangs.[1,2,4–10] That is, a birds-eye view of the surface morphology that ignores the porosity inside the bulk of the film. The vertical direction of this landscape does not scale the same way as the lateral direction. It is therefore not a self-similar surface but rather a self-affine surface.[11]

An important feature of the dynamic scaling[12,13] of a self-affine surface is that the height-height correlation function, which is defined as, $H(\mathbf{r},t)=\langle[h(\mathbf{r},t)-h(\mathbf{0},t)]^2\rangle$ has the form $r^{2\alpha}$ for $r<\xi$, and reaches a constant value of $2\omega^2$ for $r>\xi$. Here h is the deviation of the height from the mean at the growth front specified by the position $\mathbf{r}$, and time t, and ω and ξ are the interface width or root mean square roughness and lateral correlation length, respectively. α is the roughness exponent (value between 1 and 0) which describes the local roughness with a larger value for a smoother surface. Both ω and ξ grow as a power law in time, $\omega\sim t^{\beta}$ and $\xi\sim t^{1/z}$, where the exponents scale as $z=\alpha/\beta$. The lateral correlation length ξ defines a length scale beyond which the surface height fluctuations are not correlated. This means that there is no long-range characteristic length scale involved, the surface height fluctuation is random beyond the correlation length.

Because of the ability of sideways growth in the normal incidence ballistic deposition model, it is believed that the surface morphological evolution (by ignoring the interior structure such as voids and overhangs) belongs to the Kardar, Parisi, and Zhang (KPZ) universality class.[4–10] This is originally described by a nonlinear continuum equation of the form[14]

$$\frac{\partial h}{\partial t}=\upsilon\nabla^2 h+\frac{\lambda}{2}|\nabla h|^2+\eta(\mathbf{r},t), \tag{1.1}$$

where $\eta(\mathbf{r},t)$ is a Gaussian noise with zero means: $\langle\eta(\mathbf{r},t)\eta(\mathbf{r}',t')\rangle=2D\delta(\mathbf{r},t)\delta(\mathbf{r}',t')$. D is the strength of the noise. In this universality class, $\beta\sim0.24$ and $\alpha\sim0.38$ and has been a subject of extensive theoretical investigation in the past.

Although this elegant model has attracted much scientific interest, realistic applications of this model in practical thin film deposition have been very rare.[1,2] One of the main differences between the model and practical thin film deposition is the directionality of the incident flux. In many common deposition techniques such as sputter deposition[15] and chemical vapor deposition,[16] and more recently the oblique angle deposition,[17–20] the incident flux direction is never restricted only to the vertical direction. Instead, the flux arrives at the surface either with a distribution of angle with respect to the surface normal, or at a particular oblique angle. An important question can be raised: would a distribution of incident flux fundamentally alter the scaling and universality behavior of the morphological evolution? In this paper, we study the effect of two particular flux distributions, namely, a cosine distribution flux (realized in sputter deposition or chemical vapor deposition) and a fixed incident flux at a large angle with respect to the surface normal (realized in oblique angle deposition), on the scaling properties of the morphological evolution of the surface. We found that the non-normal incidence flux produces a dramatic change in the dynamics of growth front. In particular, we found that a characteristic length scale is generated in the surface morphology that would lead to a breakdown in dynamic scaling.

Our ballistic deposition is based on on-site lattice simulation where particles shower down onto a two-dimensional surface that is initially flat. The particles will stick upon first nearest-neighbor contact. The dimension of the simulation is 4096×4096 lattice units with periodic boundary conditions. For a measure of deposition time, we use the number of deposited particles per unit area (n/A). This is just the total number of particles deposited onto the film divided by the total area of the substrate. To establish a baseline of our simulation, we first performed a conventional ballistic deposition where the incidence flux is dropped down normal to the surface, shown as the inset in Fig. 1(b). In Figs. 1(a) and

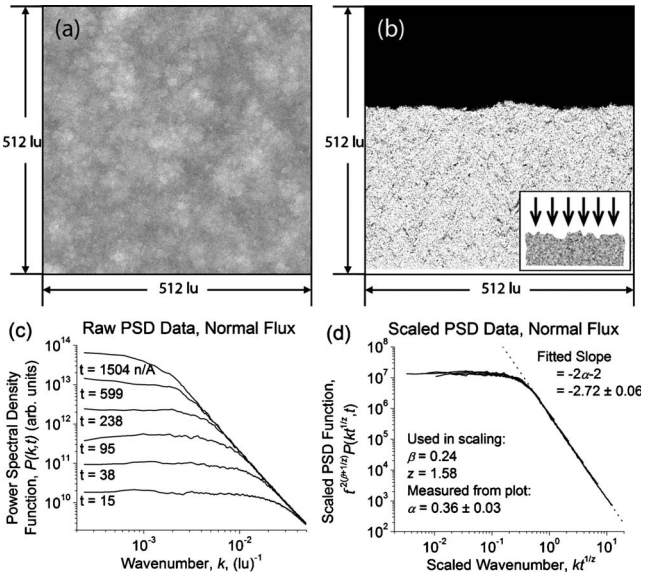

FIG. 1. Results from normal incident flux simulations. (a) Top view of the surface at a deposition time of 95 n/A. The images cover a reduced area of 512×512 lattice units. (b) Cross-section view of the film at the same time and scale. The inset shows a schematic of the flux distribution. (c) PSD function curves of the surface over the course of the simulation. (d) PSD data from (c) after scaling. The scaling exponents used are $\beta=0.24$ and $z=1.58$, giving a vertical scaling factor of $t^{-2(\beta+1/z)}=t^{-1.75}$, and a horizontal scaling factor of $t^{1/z}=t^{0.633}$. The value $\alpha=0.36\pm0.03$ is measured from the tail of the resulting collapsed plot using the equation $\alpha=-(\text{slope}+2)/2$.

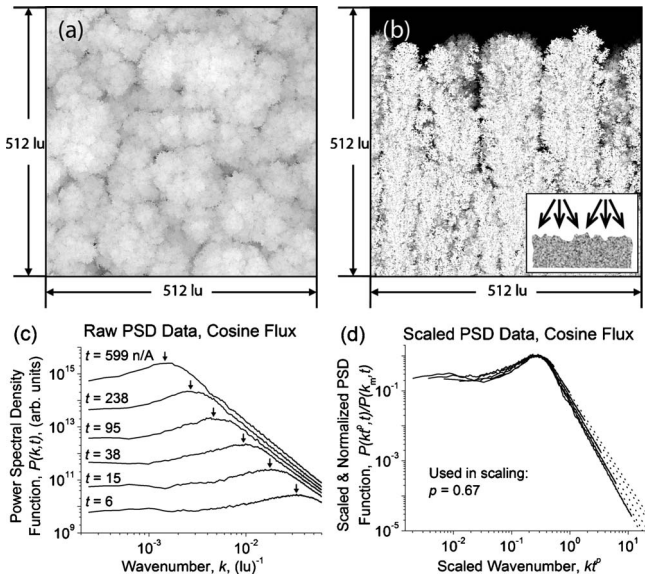

FIG. 2. Results from cosine incident flux simulations. (a) Top view of the surface at time 95 n/A. The images cover a reduced area of 512×512 lattice units. (b) Cross-section view of the film at the same time and scale. The inset shows a schematic of the flux distribution $\sim\cos(\theta)$, where θ is the flux angle with respect to the surface normal. (c) PSD function curves of the surface over the course of the simulation. Vertical arrows indicate the PSD peaks. (d) PSD data from (c) after scaling. First the curves were normalized as $P(k,t)/P(k_m,t)$. Then the curves were scaled horizontally using a scaling factor of t^p with $p=0.67$. The dotted lines show linear extensions of the tails of the final curves.

1(b) we show the morphology of the surface at time 95 n/A. To study the characteristics of the surface, it is convenient to measure the power spectral density (PSD) function of the surface at different time during the simulation. These are shown in Fig. 1(c). The PSD, $P(k)$, of a self-affine surface can be described as $P(k)=\omega^2\xi^2g(k\xi)$,[21] where k is the wave vector along the surface and $g(x)=1$, for $x\ll1$ and $g(x)=x^{-2\alpha-2}$, for $x\gg1$. Upon rescaling, the PSD profiles collapse into one universal curve as shown in Fig. 1(d). The β and z used in the scaling, 0.24 and 1.58, respectively, are those given in literature for the KPZ universality class. The α extracted from the tail part of the scaled profile gives $\alpha\sim0.36\pm0.03$, a value close to the 0.38 reported in the literature in the KPZ universality class.[1,2] The degree to which the curves successfully collapse supports that normal incidence ballistic deposition falls into this universality class as claimed in the literatures.[4–10]

With the baseline established, we now simulate the morphological evolution of a cosine incident flux, as shown as the inset in Fig. 2(b). This distribution is defined such that the probability of the particle launching from the source is proportional to $\cos\theta$, where θ is the incident flux angle as measured with respect to the surface normal. In a discrete model, the cosine distribution can be obtained by assigning each particle a velocity vector (specified in spherical coordinates, θ, φ) based on the formulas, $\theta=\arcsin(x^{1/2})$, and $\varphi=2\pi x$, where θ is the oblique angle, φ is the azimuthal angle, and x is a uniform random number from 0 to 1.[22]

In non-normal incident ballistic deposition, the incident flux of material that strikes the surface with an oblique angle is preferentially deposited onto the top of surface features with larger height values. The areas behind these features get shadowed and voids are formed. In Figs. 2(a) and 2(b) we show the morphology of the resulting surface after a deposition time of 95 n/A. The PSD profiles for various times are shown in Fig. 2(c). A characteristic wave vector, k_m, appears as a bump in each of the profiles, which indicates that wavelength selection occurs during the deposition. To check for dynamic scaling, we want to rescale the profiles in such a way that the peaks of the curves coincide. This is a two-step process involving first vertically normalizing the curves and then horizontally scaling them using a scaling factor. In Fig. 3(a) we show the time evolution of $1/k_m$ on a log-log scale. The slope of the linear fit to these $1/k_m$ values is $\sim0.67\pm0.04$, and is taken as the scaling factor exponent. In Fig. 2(d), we show the normalized and scaled curves. It is seen that while the curves do collapse significantly, they remain distinct and do not form a single universal curve. Self-affine scaling is not achieved. In addition, the α extracted from the tails of the curves is not constant, and increases over time, as seen in Fig. 3(b). Increasing of α implies a decrease in local surface roughness over time. Increasing of α was also observed by a 2D oblique angle ballistic deposition simulation.[23]

Wavelength selection also occurs in a solid on a solid (SOS) model when a cosine incident flux is assumed.[24] In a SOS model, particles launched onto the sidewalls do not

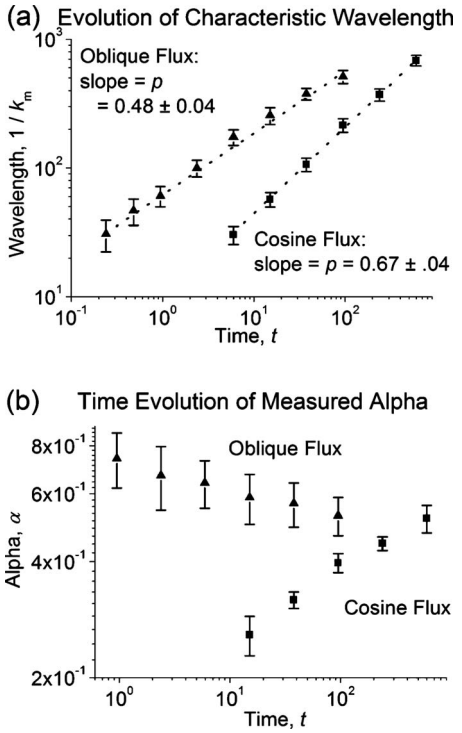

FIG. 3. Time evolution of non-normal incident flux simulation features. (a) Characteristic wavelength, $1/k_m$, evolution is plotted on a logarithmic scale for both non-normal cases, cosine incident flux (filled squares) and oblique flux (filled triangles). The slopes of the linear fits are used as the scaling exponent in Figs. 2 and 4, and are found to be 0.67 ± 0.04 and 0.48 ± 0.04, respectively. (b) The values of α measured from the tails of the distinct curves in Figs. 2(d) and 4(d). Nonconstant values indicate the breakdown of dynamic scaling in both cases.

stick but slide down to the bottom. Sidewall growth is therefore not included. No overhangs are formed and no pores are generated in the film. Our present results demonstrate that by allowing the sidewall growth in the ballistic deposition, it does not eliminate the wavelength selection. [However, the value of the growth exponent β is estimated to be ~ 0.6 for the ballistic deposition with cosine incident flux. This value is quite different from that obtained by the solid-on-solid model which is ~ 1.[24] This is due to the fact that the ballistic deposition model allows sidewall growth and tends to smooth the surface.] Wavelength selection is purely generated by the shadowing effect[23,25–27] due to a non-normal incident flux. Wavelength selection has been observed frequently in sputter deposition[28] and chemical vapor deposition of films.[29]

Recently there has been intense interest in another deposition technique called oblique angle deposition.[17–20] In this deposition technique the incident flux makes an angle θ with respect to the surface normal. For $\theta > 80°$, it is called "glancing angle deposition."[18] This distribution can be seen as the inset in Fig. 4(b). Because of the extreme shadowing, isolated nanostructures can be formed. Here we simulate the morphological evolution of a particular incident angle, namely, $\theta = 87°$ from all azimuthal directions with respect to the surface normal. (The results obtained from this flux distribution are similar to that obtained in the glancing angle deposition with a fixed incident flux angle while rotating the substrate.) The results of the simulations are shown in Fig. 4. It is seen that the structures are more isolated with the existence of large gaps and voids in between columns consistent with experimental observations.[17–20] A clear k_m also appears in the PSD profiles. In Fig. 3(a) we show the time evolution of $1/k_m$ (filled triangles) on a log-log scale. The slope of the linear fit to these $1/k_m$ values is $p \sim 0.48 \pm 0.04$, consistent with recent experimental findings.[19,20] Again the α extracted from the tails of the scaled curves is not constant, decreasing over time, as seen in Fig. 3(b). This contrasts the increasing α value for the cosine flux distribution case. Decreasing of α implies an increase in local surface roughness over time.

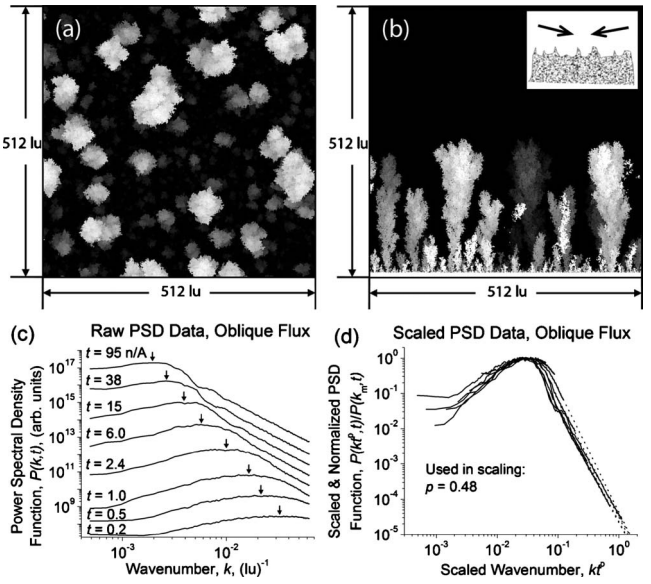

FIG. 4. Results from $\theta = 87°$ incident flux simulations. (a) Top view of the surface at time 6 n/A. (b) Cross section view of the film at the same time and scale. The inset shows a schematic of the flux distribution, $\theta = 87°$. (c) PSD function curves of the surface over the course of the simulation. Vertical arrows indicate the PSD peaks. (d) PSD data from (c) after scaling. The scaling process was the same as in Fig. 2 but with $p = 0.48$. The dotted lines show linear extensions of the tails of the final curves.

It is also of interest to examine more closely how the wavelengths, λ, of these surfaces evolve over time. Since $\lambda \sim 1/k_m$, we can see from Fig. 3(a) again that the wavelength exhibits a linear behavior, indicating that the growth can be put in the form $\lambda \sim t^p$, where the exponent p for these two cases is equal to the respective slopes. It has been argued,[28] based on a needle model, that the value of p should be $\frac{1}{2}$. In our case of $\theta = 87°$ flux, $p \sim 0.48 \pm 0.04$, which is close to the value $\frac{1}{2}$, but the case of the cosine flux gives $p \sim 0.67 \pm 0.04$, which is significantly different from the expected value. However, the needle model does not include the possibility of lateral correlation while ours does. This may turn out to be a key difference between the needle model and ballistic cosine distribution flux model, especially for the cosine distribution flux case. It should be noted that it is unclear at this point if there should even be a universal value for p, though simulations using solid-on-solid rules

have also shown agreement with a universal $p=0.5$.[24] Whether ballistic deposition with a cosine distribution may belong to a different universality class, or that p may not have universality behavior at all is something that will need to be determined through further modeling and experimentation.

Finally, we briefly mention about the breakdown of scaling in the cosine distribution case and how it relates to the growth of the surface wavelength and correlation length. We have calculated the exponent associated with the lateral correlation length from the height-height correlation function and found that it is 0.65 ± 0.03 which is slightly different compared to the exponent associated with the wavelength. If they are exactly the same the PSD should scale and the value of α should not change as a function of time. Note that the difference between the exponents associated to the wavelength and lateral correlation length in the solid on solid model is more obvious.[24] This is probably because in the case of solid on solid model the fluctuations in height are much more severe and difference between the two length scales is more dramatic. For our case of ballistic deposition, the overhang structure tends to smooth the surface and the difference between the two length scales becomes more subtle. The breakdown of the scaling behavior is more easily visualized using PSD analysis.

In conclusion, we have given further evidence supporting the assertion that a ballistic deposition model with normal incident flux belongs to the KPZ universality class. We have also shown that the same model with a non-normal incident flux ceases to belong to that class. In fact, the surface is no longer self-affine and does not follow the usual dynamic scaling hypothesis. This continues to be the case for the oblique angle flux. Finally while we have shown that the characteristic wavelength created by both cosine and oblique angle fluxes do indeed scale with time according to $\lambda \sim t^p$, we cannot make any conclusion regarding the universality value of p.

The work is partially supported by NSF REU under Program No. 0850934, NSF NIRT under Grant No. 0506738, and Rensselaer URP (Undergraduate Research Participation) Program.

[1] A.-L. Baraba′si and H. E. Stanley, *Surface Growth* (Cambridge University Press, Cambridge, England, 1996), p. 19.
[2] P. Meakin, *Fractals, Scaling and Growth Far from Equilibrium* (Cambridge University Press, New York, 1998), p. 440.
[3] M. J. Vold, J. Colloid Sci. **14**, 168 (1959).
[4] Y. P. Pellegrini and R. Jullien, Phys. Rev. Lett. **64**, 1745 (1990).
[5] H. Yan, D. Kessler, and L. M. Sander, Phys. Rev. Lett. **64**, 926 (1990).
[6] J. Yu and J. G. Amar, Phys. Rev. E **65**, 060601 (2002).
[7] F. D. A. Aarão Reis, Physica A **364**, 190 (2006).
[8] C. A. Haselwandter and D. D. Vvedensky, Phys. Rev. E **73**, 040101 (2006).
[9] F. D. A. Aarão Reis, Phys. Rev. E **63**, 056116 (2001).
[10] F. D. A. Aarão Reis, Phys. Rev. E **69**, 021610 (2004).
[11] B. B. Mandelbrot, Phys. Scr. **32**, 257 (1985).
[12] F. Family and T. Vicsek, J. Phys. A **18**, L75 (1985).
[13] F. Family, Physica A **168**, 561 (1990).
[14] M. Kardar, G. Parisi, and Y. C. Zhang, Phys. Rev. Lett. **56**, 889 (1986).
[15] J. Mahan, *Physical Vapor Deposition of Thin Films* (Wiley, New York, 2000).
[16] *Principles of Chemical Vapor Deposition*, edited by D. M. Dobkin and M. K. Zuraw (Springer, New York, 2006).
[17] Akhlesh Lakhtakia and Russell Messier, *Sculptured Thin Films: Nanoengineered Morphology and Optics*, SPIE Press Monograph Vol. 143 (Bellingham, Washington, 2005).
[18] M. Hawkeye and M. J. Brett, J. Vac. Sci. Technol. A **25**, 1317 (2007).
[19] F. Tang, T. Karabacak, L. Li, M. Peliccione, G.-C. Wang, and T.-M. Lu, J. Vac. Sci. Technol. A **25**, 160 (2007).
[20] K. Kaminska, A. Amassian, L. Martinu, and K. Robbie, J. Appl. Phys. **97**, 013511 (2005).
[21] M. Pelliccione and T.-M. Lu, *Evolution of Thin Film Morphology—Modeling and Simulations* (Springer, New York, 2008), p. 39.
[22] J. Greenwood, Vacuum **67**, 217 (2002).
[23] J. Yu and J. G. Amar, Phys. Rev. E **66**, 021603 (2002).
[24] M. Pelliccione, T. Karabacak, and T.-M. Lu, Phys. Rev. Lett. **96**, 146105 (2006).
[25] R. Messier, J. Vac. Sci. Technol. A **4**, 490 (1986).
[26] C. Tang, S. Alexander, and R. Bruinsma, Phys. Rev. Lett. **64**, 772 (1990).
[27] J. H. Yao and H. Guo, Phys. Rev. E **47**, 1007 (1993).
[28] M. Pelliccione, T. Karabacak, C. Gaire, G.-C. Wang, and T.-M. Lu, Phys. Rev. B **74**, 125420 (2006).
[29] G. T. Dalakos, J. P. Plawsky, and P. D. Persans, Phys. Rev. B **72**, 205305 (2005).